Optical performance of solar modules

Jo Gjessing[a]*, Erik S. Marstein[a]

[a]Institute for Energy Technology, Instituttveien 18, 2007 Kjeller, Norway

Abstract

Encapsulation of a solar cell affects its optical performance, a fact that is often overlooked when the efficiency of different types of solar cells is compared. In this work we have measured the reflectivity of silicon wafers with textures typically applied in the industry, i.e. random pyramids and isotropic texture with conventional silicon nitride anti-reflex coatings, as well as a graded porous silicon anti-reflection coating. We investigate how the reflectivity is affected by angle of incidence for all surfaces both with and without encapsulation. The reflectivity of the random pyramidal structure is compared with a ray-tracing model, and we achieve good correspondence both with and without encapsulation for various angles of incidence. The ray-tracing model allows us to do a complete optical loss analysis of the solar module. We apply this loss analysis methodology to four different configurations, and show that encapsulation does not necessarily imply a large optical loss, particularly when we consider higher angles of incidence.

1. Introduction

The transition from a solar cell to an encapsulated solar cell, i.e. a solar module, has a huge impact on the optical performance of the device. Not only does the reflectance at normal incidence change, but the optical performance at higher angles of incidence also changes significantly compared to that of the unencapsulated solar cell. This is an important fact that is easily ignored when comparing efficiency of silicon solar cells with different textures, and a fact that strongly affect energy yield and field performance.

It is well known that the random pyramid texture exhibits very low reflectance at normal incidence, and it is therefore preferred to the isotropic etch commonly used for multicrystalline silicon. However, it

---

* Corresponding author. Tel.: +47 6380 6637
E-mail address: jo.gjessing@ife.no

has been shown that the reflectance of the random pyramids at higher angles of incidence increases more than the reflectance of other textures such as inverted pyramids and honeycomb textures [1]. When the structures are encapsulated, the differences in reflectance between the structures are reduced, and additionally, their angular behavior follows a similar trend resembling that of the glass front side [2].

In this work we measure the angular reflectance of a graded porous silicon (PSi) anti-reflex coating (ARC) and of textures typical for monocrystalline and for multicrystalline silicon, i.e. pyramid texture and isotropic dimple texture respectively, the latter textures covered with a conventional silicon nitride (SiN$_x$) ARC. We then compare the reflectance both before and after encapsulation. To extend the loss analysis beyond the measured reflectance, we make a ray-tracing model of the random pyramid structure. The model is validated, both with and without encapsulation, with the measured reflectance spectra at normal as well as higher angles of incidence. From the ray-tracing model we are able to quantify the different optical loss mechanisms. Finally, we use the model to predict the optical performance of a solar module with a low iron glass and glass with ARC.

2. Experimental

2.1. Sample preparation

Standard random pyramid and isotropic textures are prepared on as-cut monocrystalline wafers. The random pyramids are formed by etching in a 1 % (wt) KOH, 4 % (wt) isopropanol solution at 78 °C for 40 min after a damage removal in 30 % (wt) KOH at 75 °C for 3 min. The isotropic etched samples are etched in a CP5-solution (10:5:2, HNO3:CH3COOH:HF) at 20-25 °C for 70 seconds. A SiN$_x$ ARC is deposited by plasma-enhanced chemical vapor deposition (PECVD) after the texturing process. The SiN$_x$ thickness is between 70 nm and 80 nm with a refractive index between 1.99 and 2.04 at 600 nm, which was determined by ellipsometry.

The PSi samples are made with electrochemical etching in a solution based on HF. The porosity determines the refractive index and is controlled directly by the current in the etching cell [3]. The porosity is varied gradually thus the refractive index ranges between that of silicon and that of air, depending on the porosity. A graded PSi ARC with a total thickness of about 150-200 nm is formed with a graded refractive index profile optimized for low reflectance. Two different PSi samples are prepared; one sample has a refractive index profile optimized against air, while the other has a refractive index profile optimized against glass.

The glass used for the encapsulation is cut into pieces of about 2.5 x 2.5 cm^2. The edges of the glass are polished and silver is deposited at the edges using thermal evaporation. The purpose of the silver is to reflect light that reaches the edges of the glass back into the sample to prevent light from escaping through the edges of the glass during reflectance measurements, as this would yield erroneous results. The samples are encapsulated with window glass from Pilkington and ethylene vinyl acetate (EVA) from Vistasolar at 132 degrees for 12 minutes using a P.Energy L036A laminator. The physical thickness of the EVA is found from microscope images of cross sections to be about 450 μm thick, while the glass is 1.9 mm thick. Optical constants for the glass are found using ellipsometry and transmission measurements, while the absorption coefficients of EVA is found from transmission measurements of a glass-EVA-glass sandwich.

2.2. Reflectance setup and methodology

Reflectance is measured with monochromatic light from 350 nm to 1200 nm using a 150 mm integrating sphere with a center mount configuration. The sample is inserted inside the sphere and rotated

to any desired angle of incidence. A quartz crystal achromatic depolarizer from Thorlabs is used in the beam path to randomize the partly polarized light from the monochromator.

The measured reflectance is weighted with the AM1.5 spectrum to yield weighted averaged reflectance. Light reflected from the rear side will also contribute to the measured reflectance for wavelengths above 950 nm. To calculate the weighted averaged front side reflectance from 350 nm to 1200 nm we need to estimate the front side reflectance above 950 nm. This is done by linearly extrapolating the measured reflectance from shorter wavelengths, typically between 850 nm to 925 nm. Here we assume that the curvature in the reflectance is negligible in region where we extrapolate the front side reflectance. This assumption usually holds as long as the extrapolation is not too close to the minimum in the reflectance curve, which is typically found at around 600 nm.

3. Reflectance measurements

Weighted averaged front side reflectance values for all three types of textures at various angles of incidence both with and without encapsulation are shown in **Fehler! Verweisquelle konnte nicht gefunden werden.** and Table 1. For the KOH and the isotropic etch we also show reflectance values without ARC in Table 1. The reflectance for the KOH texture is with incidence along the [100] direction. The azimuth angle did not influence reflectance for the other textures.

The data presented in Table 1 shows that the PSi has a reflectance comparable to the random pyramids at normal incidence without encapsulation. For the encapsulation samples the difference between the two structures increases. Moreover, the angular behavior of the PSi sample is not as good as the KOH and particularly the isotropic texture without encapsulation. This is not surprising given the fact that the PSi sample behaves more like a planar ARC and does not have the benefit of the other textures with multiple reflections on the surface.

The difference between the random pyramids and the isotropic texture, both with ARCs, is reduced from about five percentage points to only about a percentage point after encapsulation. Moreover, we observe that the effect of incidence angle on the encapsulated samples follow a similar trend for all samples even though their angle of incidence behavior differ greatly without encapsulation. This agrees well with literature [2] where such a behavior is attributed to the change in incidence angle on solar cell surface due to the presence of glass. The glass will refract light at grazing incidence to around 40 degrees on the solar cell surface. As a consequence, the angular performance is mostly dependent on the glass front side where the largest span of incidence angles occurs.
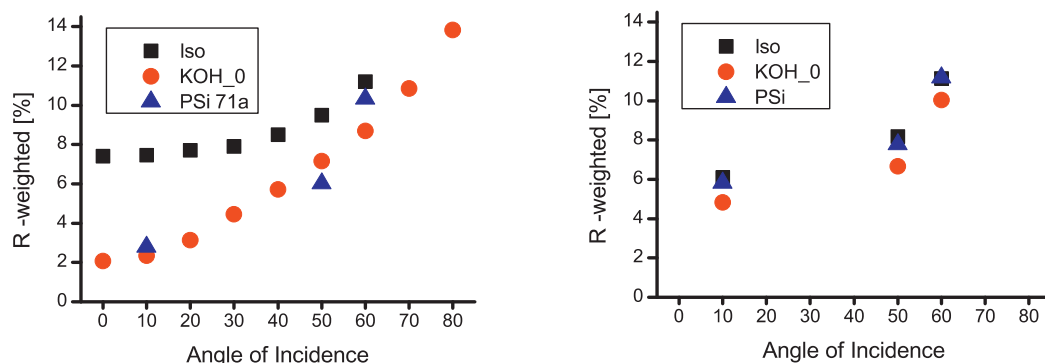

Fig. 1. AM1.5 weighted front side reflectance (350-1200 nm) for KOH texture, isotropic texture and porous silicon (PSi) texture for unencapsulated (left) and encapsulated (right) samples. Reflectance for the KOH texture is measured along the [100] direction

Table 1. AM1.5 weighted front side reflectance (350-1200 nm). Reflectance for the KOH texture is measured along the [100] direction.

Structure	Unencapsulated [%]		Encapsulated [%]	
	10 deg	60 deg	10 deg	60 deg
Isotropic w/ARC	7.5	11.2	6.1	11.1
KOH w/ARC	2.4	8.7	4.8	10.0
PSi*	2.8	10.3	5.8	11.2
Isotropic w/o ARC	26.9	29.3	9.8	15.8
KOH w/o ARC	10.8	27.9	7.1	12.0

*1 mm microscope slide used as encapsulation material. The rest of the structures use 1.9 mm window glass. The PSi sample with encapsulation is optimized for operation under glass, and is not the same as the unencapsulated sample.

4. Optical model and loss analysis

4.1. Optical model

To identify and compute the optical losses for encapsulated solar cells we make a ray-tracing model of the random pyramids using the software package TracePro [4]. The model is created by randomly displacing a regular grid of upright pyramids with a unit cell size consisting of about 15 by 15 pyramids. The model includes ARC as well as encapsulation layers of glass and EVA. The ray-tracing model outputs reflectance and absorption in the different materials as a function of wavelength. This is used for the optical loss analysis where we define the optical loss as the fraction of the light that is not contributing to excitation of charge carriers, but is rather reflected or absorbed in different parts of the solar cell and encapsulation materials. Finally, the spectral optical losses are weighted against the AM1.5 solar spectrum in the wavelength range 350-1200 nm to quantify the optical losses as a percentage value.

To make a loss analysis over the whole solar spectrum, including the longer wavelengths, we need to consider the optical properties of the rear side. We extract the rear side reflectance from analysis of internal quantum efficiency (IQE) of solar cells using the software Lassie from PV-tools [5], which is based on the method described in Ref. [6]. We find that our screen-printed aluminum reflector exhibits a Lambertian scattering behavior with a rear reflectivity of 70 %. Free carrier absorption is not included directly in this model, but rather indirectly by yielding a slightly lower rear side reflectance than if free carrier absorption was included.

We apply the loss analysis from our optical model to four different configurations at two angles of incidence, i.e. 10 degrees and 60 degrees with azimuth angle along the [100] direction. The first case is a solar cell without encapsulation, while the other three are encapsulated solar cells with 1.9 mm thick window glass, 3 mm thick low iron glass, and 3 mm thick low iron glass with ARC, respectively. We use an ideal 140 nm thick ARC in the optical model with a refractive index of 1.22. All configurations have a SiN_x ARC on the silicon surface with a thickness of 70 nm and refractive index of 2.04 at 600 nm. The thickness of the silicon wafer is set to 170 µm. The shadowing effect from metallization is not included in the loss analysis.

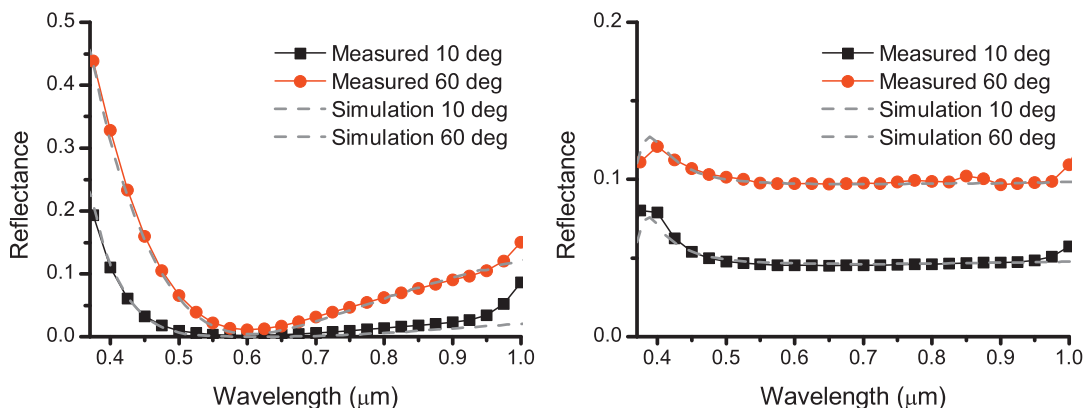## 4.2. Validation of optical model

Fig. 2. Measured and simulated reflectance shown for unencapsulated (left) and encapsulated (right) sample. Each figure shows reflectance at 10 and 60 degrees. The azimuthal angle is along the 100-plane.

Fig. 2 shows a comparison between measured reflectance and reflectance from the optical model at 10 and 60-degree angle of incidence. Here 1.9 mm thick window glass is used for encapsulation (Fig. 2, right), while the SiN_x ARC is 78 nm thick with a refractive index of 2.04 at 600 nm. The match between simulation and measurement is good, as shown in the figure, except for some deviation for the shortest wavelengths. The simulation data is also in good agreement with other ray-tracing models from the literature [7] (not shown). The long wavelength deviation derives from the onset of rear side reflectance, which is not included in this particular simulation, while the reason for the short wavelength deviation is not completely understood. We believe it might be caused by the presence of a phosphorous-doped emitter in the measured samples that is not considered in the ray-tracing model. However, the amount of solar photons in this wavelength range is quite small so that the overall effect on the calculated reflectance is not significant.

4.3. Loss analysis

Fig. 3 shows the AM1.5 weighted optical losses for the four different configurations described in section 4.1. At near normal incidence the unencapsulated cell is at advantage due to relatively low reflectance and no parasitic absorption in the glass or EVA. It is worth noticing however that the configuration with low iron glass with ARC has a slightly lower reflectance than the unencapsulated cell. It is also clear that normal window glass will absorb a significant share of the light, particularly due to higher absorption in the infrared region (not shown).

At 60-degree angle of incidence the reflectance losses increase for all structures, but they increase the least for the glass with an ARC. In fact, such a module achieves a higher generation current than an unencapsulated solar cell.
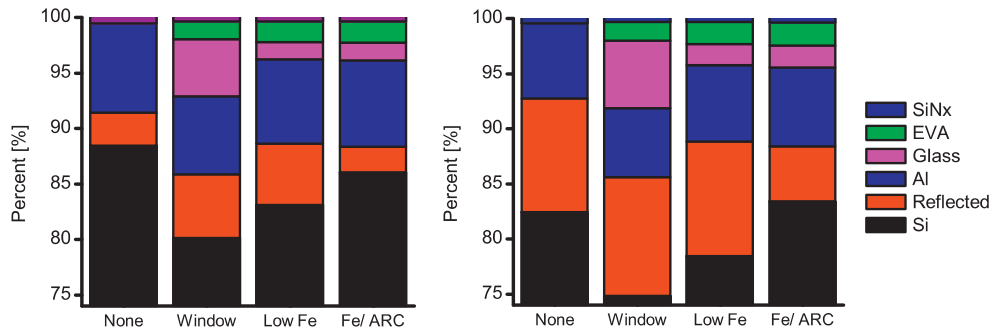
Fig. 3: Absorption in silicon together with optical losses at 10 degree incidence (left) and 60 degree incidence (right) for the following configurations: unencapsulated, 1.9 mm window glass, 3 mm low iron glass, and 3 mm low iron glass with a front side ARC.

5. Conclusion

We have measured reflectance as a function of incidence angle for silicon wafers with surface structures with and without encapsulation. The random pyramids and PSi exhibited significantly lower reflectance then the isotropic dimple structure at normal incidence without encapsulation. At higher angles of incidence the difference between the structures is reduced, and the textured samples show a better angular behaviour than the planar PSi sample. With encapsulation, the difference between the structures is significantly reduced, and all structures show a similar angular performance.

We made a ray-tracing model for the pyramidal texture that we validate with the measured reflectance. We use the model to quantify optical losses in a solar cell using different encapsulation schemes and at various angles of incidence. Particularly, we show that an ARC on the front side of the glass significantly reduce reflectance losses at normal incidence and that the effect is even more pronounced at higher angles of incidence compared to glass without ARC.

Acknowledgements

References

[1] A. Parretta, A. Sarno, P. Tortora, H. Yakubu, P. Maddalena, J. Zhao, and A. Wang, "Angle-dependent reflectance measurements on photovoltaic materials and solar cells," *Optics communications*, vol. 172, no. 1–6, pp. 139–151, 1999.

[2] J. Balenzategui and F. Chenlo, "Measurement and analysis of angular response of bare and encapsulated silicon solar cells," *Solar Energy Materials and Solar Cells*, vol. 86, no. 1, pp. 53–83, Feb. 2005.

[3] J. H. Selj, A. Thøgersen, S. E. Foss, and E. S. Marstein, "Optimization of multilayer porous silicon antireflection coatings for silicon solar cells," *Journal of Applied Physics*, vol. 107, no. 7, p. 074904, 2010.

[4] "TracePro, www.lambdares.com."

[5] "www.pv-tools.de/."

[6] R. Brendel, M. Hirsch, R. Plieninger, and J. H. Werner, "Ouantum Efficiency Analysis of Thin-Layer Silicon Solar Cells with back surface fields and optical confinement," in *IEEE Trans. Electron. Dev.*, 1996, vol. 43, no. 7, pp. 1104–1113.

[7] S. C. Baker-finch and K. R. Mcintosh, "Reflection of normally incident light from silicon solar cells with pyramidal texture," *Prog. Photovolt: Res. Appl.*, vol. 19, pp. 406–416, 2011.